ICARUS 60, 391–403 (1984)

Radar and Photoelectric Observations of Asteroid 2100 Ra-Shalom

STEVEN J. OSTRO[1]

Department of Astronomy, Cornell University, Ithaca, New York 14853

ALAN W. HARRIS

Jet Propulsion Laboratory, California Institute of Technology, Pasadena, California 91109

DONALD B. CAMPBELL

National Astronomy and Ionosphere Center,[2] Arecibo, Puerto Rico 00613

IRWIN I. SHAPIRO

Harvard–Smithsonian Center for Astrophysics, Cambridge, Massachusetts 02138

AND

JAMES W. YOUNG

Table Mountain Observatory, Jet Propulsion Laboratory, California Institute of Technology, Pasadena, California 91109

Received February 1, 1984; revised June 15, 1984

Results of 13-cm-wavelength radar observations and V-filter photoelectric observations of Ra-Shalom during its 1981 Aug–Sep apparition are reported. The radar data yield detections of echoes in the same sense of circular polarization as transmitted (i.e., the SC sense) as well as in the opposite (OC) sense. The estimate of the ratio of SC to OC echo power, $\mu_c = 0.14 \pm 0.02$, indicates that most, but certainly not all, of the backscattering is due to single reflections from surface elements that are fairly smooth at decimeter scales. The value obtained for the OC radar cross section on Aug 26 (1.2 ± 0.3 km^2) is about three times larger than those obtained on Aug 23, 24, and 25. The echo bandwidth appears to be within about 1.5 Hz of 5.0 Hz on each date. The photoelectric data suggest a value, $P_{syn} = 19.79$ hr, for the synodic rotation period, and yield a composite lightcurve with two pairs of extrema. Combining this value for P_{syn} with a firm lower bound (4 Hz) on the maximum echo bandwidth yields a lower bound of 1.4 km on the maximum distance between Ra-Shalom's spin axis and any point on its surface.

I. INTRODUCTION

Ra-Shalom is one of the four known members of the Aten class of Earth-crossing asteroids (Shoemaker *et al.*, 1979) and is further distinguished by the shortest semimajor axis (0.832 AU) of any numbered minor planet.

Radiometric, polarimetric, and UBV photometric measurements (Lebofsky *et al.*, 1978, and references therein) were conducted shortly after the object's 1978 Sep 10 discovery (Helin *et al.*, 1978). Lebofsky *et al.* (1978) argued that the "standard," low-thermal-inertia model yielded albedo and diameter estimates that were at odds with those derived from UBV colors and polarimetry. They resolved this discrepancy by adopting a "nonstandard," high-thermal-inertia (i.e., "bare rock") model (introduced previously to handle a similar discrepancy for 1580 Betulia) which, when

[1] Current address: Jet Propulsion Laboratory, California Institute of Technology, Pasadena, Cailf. 91109.

[2] Operated by Cornell University under contract with the National Science Foundation and with support from the National Aeronautics and Space Administration.

0019-1035/84 $3.00

coupled with their 10-μm data, yielded estimates for Ra-Shalom's diameter (3.42 $\pm$ 0.18 km) and geometric albedo (p_v = 0.040 $\pm$ 0.004). More extensive radiometric observations (at 5 and 20 μm as well as at 10 μm) during Ra-Shalom's 1981 apparition support the high-thermal-inertia model and yield a diameter of about 3 km (Lebofsky *et al.*, 1984).

In this paper we report radar and photoelectric observations of Ra-Shalom conducted during its 1981 apparition. Our results provide constraints on the asteroid's size, shape, spin vector, and surface properties.

II. RADAR OBSERVATIONS

We used the Arecibo Observatory's 2380-MHz (λ 13 cm) radar system to observe Ra-Shalom on the four dates: 1981 Aug 23–26 (UT), completing a total of 72 transmit/receive cycles, or "runs." For each run, we received either the *same* rotational sense of *circular* polarization as transmitted (i.e., the "SC" sense), or the opposite ("OC") sense. Since the handedness of a circularly polarized wave is reversed upon normal reflection from a smooth dielectric interface, the OC sense dominates echoes from planetary surfaces that look sufficiently smooth at the observing wavelength. (A single dielectric interface with minimum radius of curvature much greater than the wavelength would fulfill this requirement.) The presence of an SC echo can result from single-reflection backscattering from interfaces that are rough at scales comparable to the wavelength, as well as from multiple scattering. The ratio, μ_c, of SC to OC echo power, is therefore an intensive (but possibly orientation-dependent) property of the target and characterizes the overall near-surface roughness.

Since Ra-Shalom's physical properties (and hence its radar echo strength) were poorly known, we restricted the first night's observations to reception in the (normally stronger) OC sense. This strategy proved successful. With an OC detection in hand, we then interleaved OC runs with single SC runs on Aug 24 and 25, and with pairs of SC runs on Aug 26. The four nights of observation produced a total of 36 OC and 36 SC echo power spectra, each consisting of 392 independent samples at 1.025-Hz intervals. The experimental techniques and data reduction procedures were nearly identical to those described by Ostro *et al.* (1983). Table I lists for each date the polarization breakdown of runs and the data acquisition intervals.

TABLE I

RADAR OBSERVATIONS

Date (1981 Aug)	Number of runs		Receive times (hr : min UT)		
	OC	SC	Start	Stop	Midpoint
23	10	0	03 : 31	04 : 41	04 : 06
24	10	10	02 : 34	04 : 40	03 : 37
25	10	12	02 : 20	04 : 43	03 : 32
26	6	14	02 : 24	04 : 38	03 : 31

Summation of the data revealed OC and SC echoes (Figs. 1, 2) that are largely, if not entirely, confined to an approximately 5-Hz band centered about 1 Hz from the ex-

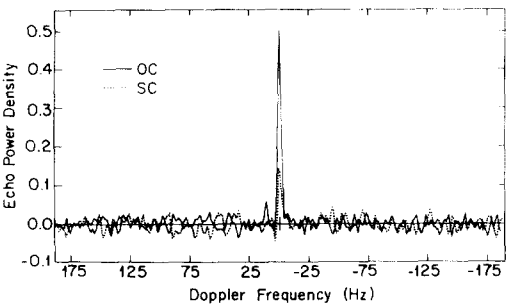

FIG. 1. Ra-Shalom's average OC and SC radar echo power spectra, smoothed to an effective resolution of 4 Hz. Echo power density, in units of km^2 of radar cross section per 4-Hz frequency resolution cell, is plotted against Doppler frequency. Each spectrum is a weighted mean of all the available spectra in the specified polarization. The vertical bar at 0 Hz indicates plus and minus one standard deviation of the background noise.

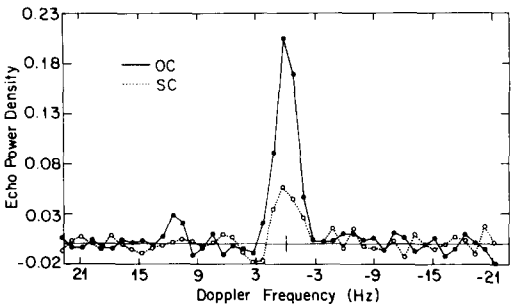

FIG. 2. Ra-Shalom's average OC and SC radar echo spectra. Echo power density, in units of km² of radar cross section per 1-Hz frequency resolution cell, is plotted against Doppler frequency. The vertical bar at 0 Hz indicates plus and minus one standard deviation of the background noise.

pected Doppler frequency. To obtain a formal estimate of this frequency offset (f_0), we fit by least squares a model of the form, $S(f) = S_0[1 - (f - f_0)^2/(B/2)^2]^{n/2}$, to the spectra in Fig. 2, with n and the full bandwidth B fixed to integral values in the ranges $2 \leq n \leq 6$ and $4 \leq B \leq 8$. The 25 resulting estimates of f_0 span the interval $-1.27 \leq f_0 \leq -1.37$, have a mean and rms dispersion of -1.32 ± 0.03, and have standard errors no greater than 0.1. Accordingly, we adopt -1.3 ± 0.2 Hz as a "safe" estimate of f_0 and its standard error. This value has been subtracted from the abscissa scales in all our plotted spectra (Figs. 1–3). Referring our measurement to a convenient epoch of echo reception (1981 Aug 25 at 02h UTC), we obtain an estimate, -18021.4 ± 0.2 Hz, for the Doppler shift of the echo for a transmitter frequency of 2380 MHz.

Echo Bandwidth, Radar Cross Section, and Polarization Ratio

Figure 3 shows our "single-night" OC spectra. Echo power at levels higher than three standard deviations of the background noise is confined to a band ≈4 Hz wide, and each spectrum drops below the one-standard-deviation level within a band ≈6 Hz wide. The maximum bandwidth, B, occupied by echoes from Ra-Shalom, is certainly at least 4 Hz, but the data alone do not preclude the possibility that $B \gg 4$ Hz. Unfortunately, the small number of echo points above the background noise leave too few degrees of freedom to obtain a statistically meaningful estimate of B by fitting a (four-parameter) "$S(f)$" model. On the other hand, stronger and more highly resolved echo spectra obtained for other small asteroids [e.g., 1685 Toro (Ostro *et*

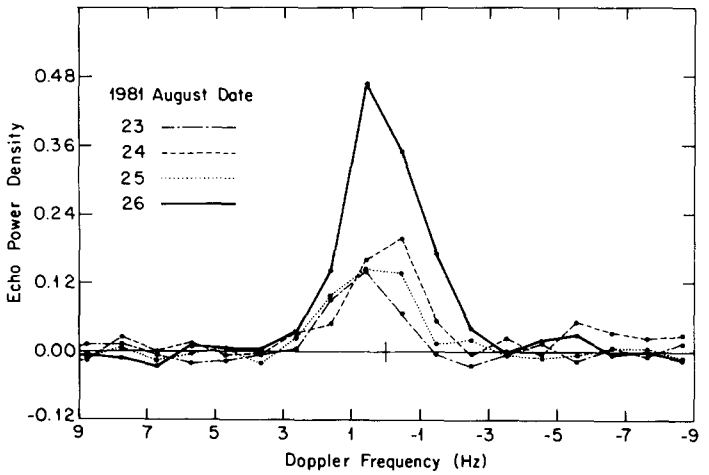

FIG. 3. Ra-Shalom's OC radar echo power spectra obtained on four dates in August 1981. Echo power density, in units of km² of radar cross section per 1-Hz resolution cell, is plotted against Doppler frequency. The standard deviation of the background noise was between 0.015 and 0.020 km² Hz⁻¹ on each night. Note the relatively high amplitude of the Aug 26 echo.

al., 1983), 1862 Apollo (Ostro *et al.*, 1981), 433 Eros (Jurgens and Goldstein, 1976)] are broad rather than sharply peaked, and have half-power bandwidths $>0.5\ B$, corresponding to $n < 5$. In this context, we consider it very unlikely that $B > 8$ Hz, and for purposes of discussion will adopt $4 \leq B \leq 8$ as a "safe" interval estimate of Ra-Shalom's maximum echo bandwidth.

Table II lists estimates of the radar cross sections (σ_{OC} and σ_{SC}) and the circular polarization ratio ($\mu_c = \sigma_{SC}/\sigma_{OC}$). The weighted mean of estimates of μ_c for Aug 24, 25, and 26 is 0.14 ± 0.02. This value is similar to Toro's (0.18 ± 0.04) and indicates that most, but certainly not all, of the echo is due to single-reflection backscattering from smooth surface elements. The variation in single-night estimates of μ_c suggests that Ra-Shalom is probably heterogeneous at decimeter scales.

Variations in spectral shape, e.g., in degree and direction of skewness, are evident in the single-night OC spectra. These may result from an irregular asteroidal figure and/or a heterogeneous surface, but more definitive statements are precluded by the small number of echo points above the noise.

The most striking feature of the comparison in Fig. 3 is the relatively high strength of the Aug 26 echo. The six OC runs on that date yielded radar cross sections (1.1, 1.0, 1.0, 1.2, 1.3, and 1.6 km^2, in chronological order) whose weighted mean (1.2 km^2) is several times larger than the weighted means (0.26, 0.49, and 0.41 km^2) obtained on Aug 23, 24, and 25, respectively. We cannot explain this extreme variation in terms of known sources of measurement error, and therefore attribute it to an intrinsic dependence of the OC radar cross section on Ra-Shalom's orientation. Such extreme variations in asteroidal values of σ_{OC} have not been seen at 13-cm wavelength but were noted for 433 Eros at 70 cm (Campbell, private communication). We note that night-to-night variations in σ_{SC} are comparatively modest; thus the circular polarization ratio was lower on Aug 26 than on Aug 24 or 25.

TABLE II

RADAR CROSS SECTIONS AND CIRCULAR POLARIZATION RATIO*

Date (1981 Aug)	σ_{OC} (km^2)	σ_{SC} (km^2)	μ_c
23	0.26 ± 0.07	No data	No data
24	0.49 ± 0.13	0.09 ± 0.04	0.18 ± 0.07
25	0.41 ± 0.11	0.12 ± 0.04	0.30 ± 0.08
26	1.19 ± 0.30	0.16 ± 0.05	0.13 ± 0.02
All available data			
Weighted mean	0.52 ± 0.13	0.12 ± 0.04	0.14 ± 0.02
Unweighted mean	0.59 ± 0.34	0.12 ± 0.03	0.20 ± 0.07

* Uncertainties assigned to σ_{OC} and σ_{SC} are the root sum square of the standard deviations in the receiver noise ($\leq$0.04 km^2) and systematic errors (estimated as 25% of the cross-section estimates). Uncertainties assigned to μ_c propagate from the noise alone and were calculated according to Appendix I of Ostro *et al.* (1983). Weighted means in Table II were calculated using statistical weights. Uncertainties assigned to unweighted means are the rms dispersions about the mean.

III. PHOTOELECTRIC OBSERVATIONS

We used the 24-in. Cassegrain reflector of Table Mountain Observatory to observe Ra-Shalom on seven nights in 1981 Aug–Sep. Table III lists for each date the asteroid's geocentric coordinates; the distances r and Δ of the asteroid from the Sun and Earth, respectively; and the solar phase angle α. Our methods of observation, magnitude calibration, and data reduction have been described elsewhere (Harris and Young, 1983). All observations on any given night were referenced to a single, nearby comparison star to minimize systematic errors due to differential extinction. Comparison stars and their V magnitudes are given in Table III. 1 Peg B is a Johnson and Morgan (1953) standard star, and SA 112-636 is a standard star from Landolt (1973, 1983). The tabulated V magnitudes of those stars are from those references. The other two comparison stars are identified by position and their tabulated magnitudes were measured with respect to 1 Peg B. The two standard stars were also observed with respect to one another and were found to differ by 0.714 ± 0.004 mag, in agreement with tabulated values.

TABLE III

PHOTOELECTRIC OBSERVATIONS[a]

Date	Geocentric coordinates	r (AU)	Δ (AU)	α (deg)	Phase-angle bisector		$\bar{V}(\alpha)$	Comparison star	Comparison V
	R.A. (1950.0) Dec				Long (1950.0) (deg)	Lat (deg)			
1978 Sep 12	23^h08^m9 −01°38′	1.195	0.188	3.20	348.0	+02.0	16.38	Unknown	—
1981 Aug 24	21 24.0 +24 29	1.159	0.180	32.09	331.7	+21.4	—	2122.6 + 2349	11.39
1981 Aug 25	21 19.3 +22 39	1.162	0.181	30.90	331.1	+20.7	17.44	2117.3 + 2159	11.35
1981 Aug 26	21 14.9 +20 49	1.164	0.182	29.86	330.5	+20.0	—	1 Peg B	9.14
1981 Aug 28	21 06.5 +17 10	1.169	0.184	28.28	329.3	+18.5	—	1 Peg B	—
1981 Aug 29	21 02.6 +15 20	1.171	0.186	27.77	328.8	+17.8	—	None used[b]	—
1981 Aug 30	20 58.9 +13 33	1.173	0.188	27.45	328.3	+17.0	—	None used	—
1981 Sep 1	20 52.0 +10 02	1.177	0.193	27.37	327.4	+15.5	17.34	1 Peg B	9.14
1981 Sep 2	20 48.9 +08 20	1.179	0.196	27.59	327.0	+14.0	—	SA112-636	9.853
1981 Sep 4	20 43.1 +05 03	1.182	0.203	27.96	326.3	+13.3	17.36	SA112-636	

[a] Observations on 1981 Aug 29 and 30 by D. Tholen, University of Arizona 61-in. telescope. Observations on 1978 Sep 12 by E. Bowell, Lowell Observatory 42-in. telescope. All others at Table Mountain Observatory 24-in. telescope. Listed for each date of observation are Ra-Shalom's geocentric equatorial coordinates, distance r from the Sun, distance Δ from Earth, the solar phase angle α, and ecliptic coordinates of the phase-angle bisector (see text). Comparison stars, their V magnitudes, and estimates of Ra-Shalom's time-averaged absolute magnitude $\bar{V}(\alpha)$ are listed for several dates. The phase angle on 1978 Sep 12 is the value at 8 hr UT near the middle of the observations. All other tabular values are for 0 hr UT.

[b] These observations were referenced directly to standard stars.

Our observations yielded a total of 194 photoelectric estimates of Ra-Shalom's V magnitude. In addition to these data, 21 estimates obtained at Lowell Observatory on 1978 Sep 12 (during Ra-Shalom's discovery apparition) have kindly been supplied to us by E. Bowell. Two data points, one each on 1981 Aug 29 and 30, were obtained with the University of Arizona 61″ telescope by D. Tholen and L. Marsteller as a part of an eight-color survey of asteroids, and were kindly provided to us by their collaborator, E. Tedesco. Table III includes information for all these observations.

The 1981 data comprise a time series that exhibits several relative extrema and a total "peak-to-valley amplitude" (Δm) of several tenths of a magnitude. In constructing a single-cycle composite lightcurve from the data, one can minimize the vertical dispersion by adjusting the synodic period P_{syn} and/or the phase relation, i.e., the variation of absolute visual magnitude with solar phase angle.

Phase Relation

The phase relation has traditionally been characterized as linear, with slope β_V given in magnitudes per degree of solar phase angle (e.g., Gehrels and Tedesco, 1979). However, the phase relations for atmosphereless bodies are known to deviate from linearity (Bowell and Lumme, 1979) at low phase angles ($\alpha \lesssim 7°$) and at high phase angles ($\alpha \gtrsim 30°$). Even within the quasilinear range ($7° \lesssim \alpha \lesssim 30°$), some theoretical phase relations exhibit modest curvature (cf. Lumme and Bowell, 1981a,b; Hapke, 1981). The 1981 photoelectric data correspond to phase angles within the interval $27.4° < \alpha < 32.1°$, so a linear phase relation can safely be used to construct a single-cycle composite. However, it might not be appropriate to use a linear approximation when matching the 1978 data ($\alpha = 3°$) to the 1981 data.

The absolute magnitude of Ra-Shalom at any given rotational phase might depend on the sub-Sun and sub-Earth latitudes, as well as on α. For example, if the asteroid were a triaxial ellipsoid with semiaxis lengths $a \geq b \geq c$ (with rotation about the c axis) and the sub-Sun and sub-Earth latitudes were positive and increasing with time, then the projected, visible, illuminated area at a given rotational phase would also increase with time. The motion of the "phase-angle bisector," a vector whose direction is the

mean of the Sun–asteroid and Earth–asteroid directions, is a convenient indicator of the changing illumination/viewing geometry (Harris *et al.*, 1984). Table III lists, for each date of photoelectric observation, the 1950.0 ecliptic coordinates of Ra-Shalom's phase-angle bisector.

Since the 1978 measurements apparently span a lightcurve minimum, a first approximation to the phase relation can be obtained by comparing the 1978 data to any set of 1981 data that span a lightcurve minimum. For example, the absolute magnitude of Ra-Shalom's lightcurve minimum on 1981 Sep 1 (at $\alpha = 27.37°$) was 17.47 mag, whereas on 1978 Sep 12 (at $\alpha = 3.20°$) it was 16.51 mag. The phase relation probably is nonlinear over this range of α. The Lumme–Bowell theory for scattering of light from particulate surfaces (Lumme and Bowell, 1981a,b) yields an approximate formula for the difference in an asteroid's absolute magnitude at two different solar phase angles, expressed as a nonlinear function of the "multiple scattering factor," Q. This parameter provides an estimate of the phase integral (q) and, when coupled with an *independent* estimate for the geometric albedo (p), provides an estimate for the Bond albedo ($A = pq$). For Ra-Shalom, the brightness estimates near epochs of minimum light yield $Q = 0.08 \pm 0.10$[3] for the multiple scattering factor.

Estimates of an asteroid's absolute magnitude[4] are usually referenced to the time-averaged, mean light level (Bowell and Lumme, 1979). (Here "mean light level" denotes time-averaged *magnitude* rather than intensity.) If we assume that the difference between minimum and mean light levels in 1978 was the same as that (0.18 mag) in 1981, then using $Q = 0.08$ to extrapolate the phase relation yields $V(0°) = 16.1 \pm 0.2$ mag, for Ra-Shalom's absolute magnitude.

Following Lumme and Bowell (1981b), we also obtain 0.034 ± 0.016[3] mag/deg for the phase coefficient β_V for a linear phase relation (Gehrels and Tedesco, 1979), using the formula $\beta_V = 0.1[V(20°) - V(10°)]$, where $V(\alpha)$ is obtained from the Lumme–Bowell model with $Q = 0.08$. Extrapolating linearly to zero phase angle gives $V(1,0) = 16.3 \pm 0.2$[3] mag. In constructing a composite lightcurve from the 1981 data, we have used a linear approximation to the Lumme–Bowell model with $Q = 0.08$, over the interval $27° < \alpha < 32°$.

Synodic Rotation Period

It was clear from an initial examination of the data that if Ra-Shalom's lightcurve has two pairs of extrema per cycle, then P_{syn} must be $\approx$14 or $\approx$20 hr. The composite lightcurves in Figs. 4b and c correspond to $P_{syn} = 13.95$ and 19.79 hr, respectively. These values were obtained by adjusting the nominal values of P_{syn} and the phase relation until the apparent vertical scatter in the data was minimized. This scatter was estimated subjectively by inspection of the plotted points.

The value $P_{syn} = 13.95$ hr results in date-

[3] The uncertainties assigned to these photometric parameters are subjective and are intended to include measurement errors as well as any systematic error introduced by the difference (~30°) between the 1978 and 1981 directions of the phase-angle bisector. In particular, in connecting the photometric results of the two apparitions, we have assumed that the difference between the 1978 and the 1981 viewing geometry introduces an error of ~0.2 mag. Since the shape, pole direction, and surface scattering properties of Ra-Shalom are unknown, the actual error could be larger. In this context, we are reluctant to make any statements about the possible physical significance of our estimates for Q and β_V.

[4] The Gehrels–Tedesco notation for absolute magnitude is $V(1,\alpha)$, or $V(1,0)$ for $\alpha = 0°$. In order to distinguish their magnitude system from the Gehrels–Tedesco system, Lumme and Bowell have dropped the "1" from their notation [$V(\alpha)$, or $V(0°)$ for $\alpha = 0°$]. Both $V(0°)$ and $V(1,0)$ are extrapolated from observations at nonzero solar phase angles. The Lumme–Bowell extrapolation to $V(0°)$ is nonlinear and is intended to provide an accurate estimate of the "true" zero-phase value. The Gehrels–Tedesco quantity $V(1,0)$ is extrapolated linearly from observations at $\alpha \geq 7°$. Since the phase relation generally is nonlinear between $\alpha = 0°$ and $\alpha = 7°$, $V(1,0)$ is not intended to be an estimator for the true zero-phase value.

to-date differences that seem excessive compared to the (predominantly systematic) errors in the photoelectric measurements. Especially disquieting are the segments from 0 to 1 hr UT and from 10 to 12 hr UT. These discrepancies could be reduced by assuming that Ra-Shalom was brightening with time due to changes in the direction of the phase-angle bisector, but then similarly large discrepancies would arise across the maximum at 7 to 10 hr UT. Doubling or tripling the value 13.95 hr still leaves several sets of data from different dates coincident in rotation phase, and yields composites with "excessive" vertical scatter at certain rotation phases (regardless of one's choice of phase coefficient or secular brightness variation).

The other nominal period, $\simeq$20 hr, proves much more satisfactory. A value, $P_{syn} = 19.79$ hr, yields a composite (Fig. 4c) in which the vertical scatter among all the points within a specified interval of rotation phase is not much larger than the scatter among the points in that interval obtained on a single date. The 1981 Aug 25 and 1981 Sep 4 data covering the maximum near 23 hr UT in Fig. 4c are separated by 12 cycles, and our final adjustments of P_{syn} were largely devoted to matching those portions of the data. We subjectively estimated the uncertainty in overlaying these curves as $\pm$20 min, corresponding to an uncertainty of $\pm$0.03 hr in P_{syn}.

Given this argument in favor of $P_{syn} = 19.79$ hr over 13.95 hr, we still must consider integer and half-integer multiples of 19.79 hr, i.e., periods corresponding to lightcurves in which the number of pairs of extrema does not equal 2. Figure 4a is composited for $P_{syn} = 9.90$ hr, and hence exhibits one pair of extrema. At 1–2 hr UT, there is an uncomfortably large ($\simeq$0.2 mag) difference between magnitudes measured on different dates. In particular, magnitudes measured on Aug 25, Aug 26, and Sep 4 are brighter than those on Aug 28 and Sep 2. Since this discrepancy is not due to a simple secular trend, we regard it as grounds for rejecting the 9.90 hr value for the period.

The possibility that $P_{syn}/n = 19.79$ hr, where n is an integer larger than unity, cannot be excluded on the basis of the photoelectric data alone. However, asteroid lightcurves with more than two pairs of extrema per cycle are extremely rare, and the number of asteroids whose lightcurves do not have two pairs of extrema per cycle decreases rapidly with increasing lightcurve amplitude, Δm. In fact, 1580 Betulia, with three pairs of extrema per cycle, is the only asteroid known to have (i) other than two pairs of extrema per cycle and (ii) $\Delta m \geq 0.3$ mag (Tedesco *et al.*, 1978). In this context we consider it unlikely (but certainly not impossible!) that $n \neq 1$. [Given the asymmetry in the 19.79-hr curve (Fig. 4c), values of P_{syn} satisfying $P_{syn} = (n + 1/2)19.79$ hr seem no more satisfactory than the value $P_{syn} = 9.90$ hr (Fig. 4a).] For the purpose of the following discussion, we adopt the provisional value, $P_{syn} = 19.79$ hr.

IV. DISCUSSION

The Ra-Shalom radar data are not adequate to yield a meaningful independent estimate of the synodic rotation period, but they do provide the following "consistency" argument in favor of $P_{syn} \approx 20$ hr. Since the estimate of σ_{OC} for Aug 26 is much higher than those for Aug 23–25, it seems likely that the subradar track on Aug 26 was not very close to those on Aug 23–25. In Figs. 4a–c, horizontal arrows indicate the rotational-phase intervals spanned by the OC radar observations for $P_{syn} =$ 9.90, 13.95, and 19.79 hr, respectively. If $P_{syn} = 19.79$ hr, then the phases observed on Aug 26 were separated by at least 45° from those on the other dates. However, if $P_{syn} = 9.90$ hr, then phases spanned by the last two OC runs on Aug 26 overlapped phases spanned by the first two OC runs on Aug 24. Forming weighted sums of these two pairs of runs, we obtain radar cross section estimates ($\sigma_{OC} = 0.7 \pm 0.2$ km^2 on the 24th and $\sigma_{OC} = 1.4 \pm 0.4$ km^2 on the

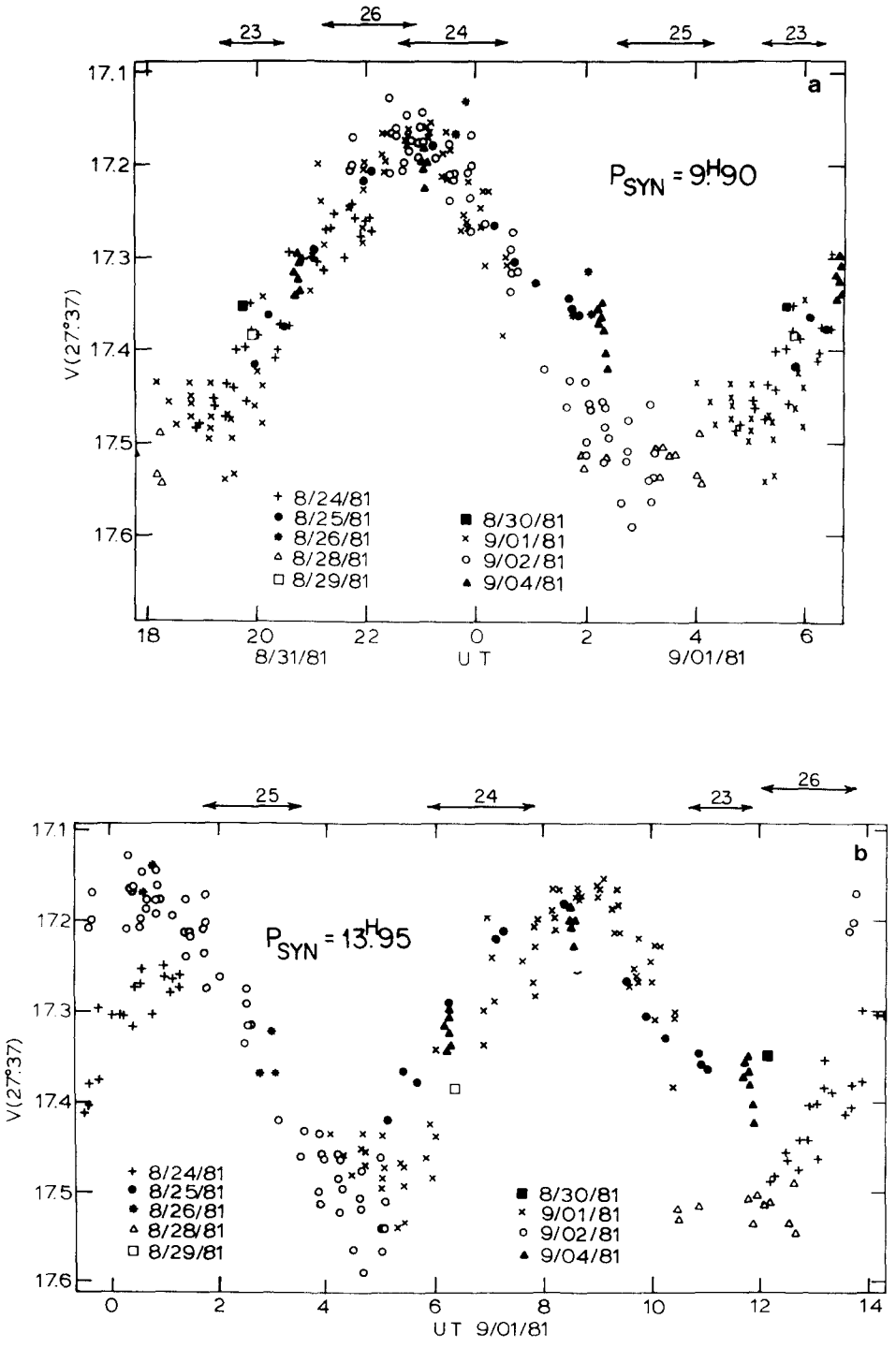

FIG. 4. Composites of Ra-Shalom's photoelectric lightcurve data, for the synodic rotation period P_{syn} equal to (a) 9.90 hr, (b) 13.95 hr, and (c) 19.79 hr. For each value of P_{syn}, horizontal arrows above the lightcurve indicate rotational phases spanned by OC radar observations on Aug 23, 24, 25, and 26. In the text we argue that $P_{syn} = 19.79 \pm 0.03$.

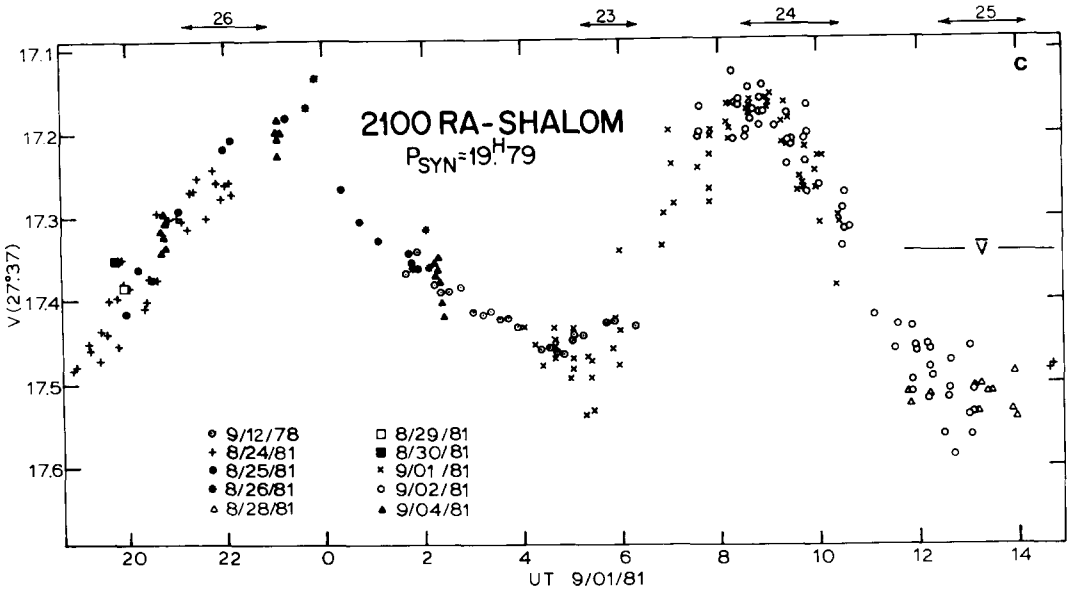

FIG. 4—*Continued.*

26th) whose difference is larger than the root sum square of our intentionally conservative estimates of the measurement errors. Similarly, if P_{syn} = 13.95 hr, then phase coverages on Aug 23 and 26 were separated by less than 5°. In short, one can conclude from Figs. 4a–c that for $P_{syn} \sim 20$ hr, the gradient in radar cross section with "longitude" is least steep. In this respect, the ensemble of radar measurements seems more compatible with a synodic period ~20 hr than ~10 or ~14 hr. (We caution that our ignorance of Ra-Shalom's shape and pole direction precludes stronger statements in support of any value of P_{syn}.)

Size and Shape

Using the value P_{syn} = 19.79 hr for the synodic period and the interval estimate, $4 \leq B \leq 8$ Hz, for the radar bandwidth, what constraints can we place on Ra-Shalom's dimensions? Noting that the radar observations sample the rotational phases corresponding to lightcurve maxima, we use an estimate of the full bandwidth, B, of the OC echo spectrum in Fig. 2 to place a lower bound on the maximum value, D_{max}, of $D = B\lambda P_{syn}/4\pi \cos \delta$. Here δ is the astrocentric declination of the radar and D is the sum of the distances, r_+ and r_-, measured from the plane containing the radar and Ra-Shalom's spin axis to those backscattering elements with the greatest positive (approaching) and negative (receding) line-of-sight velocities relative to the radar. In different words, D is the breadth, measured normal to the radar line of sight, of Ra-Shalom's polar silhouette (Ostro and Connelly, 1984). By letting $\delta = 0$, we may convert our lower bound of 4 Hz on B into a lower bound of 2.9 km on D_{max} and, hence, a lower bound of 1.4 km on the maximum distance between Ra-Shalom's spin axis and its surface, independent of assumptions about Ra-Shalom's shape. [See Ostro *et al.* (1983) for detailed discussion.]

We now attempt to obtain more elaborate, "shape dependent" constraints on Ra-Shalom's dimensions. Let us assume that Ra-Shalom is a triaxial ellipsoid with semiaxis lengths $r_{max} = D_{max}/2 = a \geq b \geq c$, where rotation is about the c axis. Figure 5 plots D_{max} vs δ for B = 4, 6, and 8 Hz. Lebofsky *et al.* (1984) have derived an infrared radiometric diameter, $D_{IR} \approx 3$ km, from 5-, 10-, and 20-μm observations of Ra-

Shalom on 1981 Aug 22 from 10:33 to 10:56 UT, with the asteroid's rotational phase within a few degrees of that corresponding to the beginning of the Aug 24 radar runs, i.e., very close to the right-hand maximum in Fig. 4c. D_{IR} is derived from an idealized spherical model (Brown *et al.*, 1982), but let us assume it equals Ra-Shalom's effective diameter, $D_{eff} \equiv (4A_{proj}/\pi)^{1/2}$, with A_{proj} the projected area of the asteroid at the time of the infrared observations. Also, let us approximate (rather crudely!) the equatorial axis ratio with $b/a = 10^{-0.4\Delta m} = 0.72$, where $\Delta m = 0.35$ mag is the lightcurve amplitude. The ratio D_{max}/D_{eff} then depends only on c/a, δ, and the rotational phase, so we may calculate D_{max} as a function of δ for several values of $c/a \leq b/a = 0.72$, as shown in Fig. 5. The stippled region is bounded on the top and bottom by contours for $c/a = 0.3$ and $c/a = b/a = 0.72$, respectively; these curves straddle that for $c/a = 0.5$. Even for $\delta = 0°$, the lower bound here on D_{max} is higher than that obtained via our first approach.

Figure 5 demonstrates graphically the constraints on Ra-Shalom's size, shape, and orientation that are provided by coupling our radar and photoelectric measurements with the IR radiometry of Lebofsky *et al.* (1984). For example, if we assume that the "true" values of D_{max} and δ correspond to a point in the stippled region, then Ra-Shalom's orientation was within ~45° of equatorial during its 1981 apparition. If the actual orientation were within a few degrees of equatorial, then values of $c/a < 0.3$ would seem unlikely, unless Ra-Shalom's radar scattering law were unusually sharply peaked. Note also that a sufficiently precise estimate of B would yield c/a as a function of δ. Of course, these statements rely on D_{IR} being a good estimate of D_{eff}; further, the curves in Fig. 5 presuppose an ellipsoidal shape.

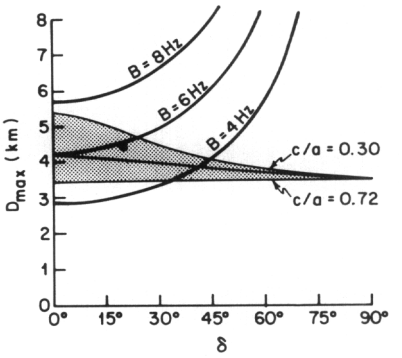

FIG. 5. Constraints on Ra-Shalom's dimensions, shape, and orientation. D_{max} is the maximum breadth of the asteroid's polar silhouette and δ is the absolute value of the average astrocentric declination of the radar during Aug 23–26, 1981. The heavy curves plot D_{max} vs δ for three values of the echo bandwidth B, assuming $P_{syn} = 19.79$ hr. Modeling Ra-Shalom as a triaxial ellipsoid with semiaxis lengths $c \leq b \leq a = D_{max}/2$, we use photoelectric and radiometric results to calculate D_{max} as a function of δ and $c/a \leq b/a = 0.72 = 10^{-0.4\Delta m}$, where $\Delta m = 0.35$ mag is the ("peak-to-valley") amplitude of the photoelectric lightcurve. The stippled region is bounded on the top and bottom by contours for $c/a = 0.3$ and $c/a = 0.72$, respectively; these curves straddle that for $c/a = 0.5$. The large dot at $\delta = 20°$, $D_{max} = 4.4$ km corresponds to the model used in Section IV to obtain estimates of Ra-Shalom's geometric albedo and surface density. (See text.)

Surface Properties

From the radar results in Table II, we can obtain estimates of Ra-Shalom's radar reflectivity and surface density. However, we also require additional assumptions about Ra-Shalom's size, shape, radar scattering properties, and orientation during the 1981 apparition.

Useful measures of an object's intrinsic radar reflectivity include the normalized OC radar cross section, $\hat{\sigma}_{OC} \equiv \sigma_{OC}/A$, where A is the target's projected area; the normalized total radar cross section, $\hat{\sigma}_T = \sigma_T/A$, where $\sigma_T \equiv \sigma_{OC} + \sigma_{SC} = (1 + \mu_C)\sigma_{OC}$; and the geometric albedo, $p \equiv \hat{\sigma}_T/4 = (1 + \mu_C)\hat{\sigma}_{OC}/4$. In general, we can write $p = \eta R$, where R is the Fresnel, normal-incidence, power-reflection coefficient and $\eta = g/4$, with g the backscatter gain (e.g., Jurdens and Goldstein, 1976, p. 5) determined by the target's shape, orientation with respect to the radar, and scattering law. [A perfect (i.e., nonabsorbing), isotropic scatterer (e.g., a metal sphere) would have $\sigma_T = A$, $g = 1$, $R = 1$, and $p = \eta = \frac{1}{4}$.]

For purposes of discussion, we model Ra-Shalom as a triaxial ellipsoid with $(a,b,c) = (2.2, 1.6, 0.9)$ km, and assume $\delta = 20°$ during the radar observations. This model corresponds to the large dot in the stippled region in Fig. 5; it is intended to be consistent with the available radar, photometric, and radiometric data. Taking into account the rotational phases of the observations on Aug 23, 24, 25, and 26, we obtain estimates of $\hat{\sigma}_{OC}$ equal to 0.04, 0.07, 0.07, and 0.2, respectively. Corresponding estimates of p are 0.01, 0.02, 0.02, and 0.05, respectively, where we have assumed the weighted mean value, $\mu_C = 0.14$, for Aug 23.

Having assumed a size, shape, and orientation, we now need to assume a scattering law to make further progress. Let us take a bistatic scattering law of the form

$$\sigma_0(\theta_i,\theta_e) = d\sigma_T/dA = 4S_0(\cos\theta_i \cos\theta_e)^k,$$

where dA is an element of surface area, θ_i and θ_e are incidence and emission angles measured with respect to the normal to dA, and S_0 and k are free parameters. This "law," first proposed by Minnaert (1941), provides a useful approximation to the light-scattering behavior of particulate surfaces (Veverka *et al.*, 1978). Although it is a physically plausible scattering law in that it satisfies the principle of reciprocity [i.e., $\sigma_0(\theta_i,\theta_e) = \sigma_0(\theta_e,\theta_i)$; Chandrasekhar (1960, pp. 94ff, 171ff)], any physical interpretation of the Minnaert parameters (S_0, k) requires additional assumptions. In particular, one is not necessarily justified in identifying S_0 with R. [See, for example, comments by Hagfors (1968, p. 263) on Evans and Pettengill (1963, p. 440).] For purposes of discussion, we assume that $S_0 = R$ for backscattering ($\theta_i = \theta_e = \theta$), so Minnaert's law reduces to $\sigma_0(\theta) = 4R\cos^{2k}\theta$, and radar observation of a normally oriented ($\theta = 0°$) surface element would yield $\hat{\sigma}_T/4 = R = p$.

For disk-integrated observations, the ratio $\eta = p/R$ is a function of k. If Ra-Shalom were uniformly bright ($k = 0.5$), η would equal unity, independent of the asteroid's shape and orientation. If Ra-Shalom were limb darkened ($k > 0.5$), the value of η would be less than unity and would depend on the asteroid's shape and orientation; so an estimate of p would provide only a lower bound on R. For example, for Lambert scattering ($k = 1$), $\eta = \frac{2}{3}$ for a sphere and $0.4 \lesssim \eta \lesssim 0.8$ for an ellipsoid with axis ratios $b/a = c/a \approx 0.4$ (French and Veverka, 1983).

Let us now attempt to estimate Ra-Shalom's density under the assumption that $R = p$. If the surface is a regolith of porous, lossless, dielectric rock, then the electrical behavior of the surface material is described entirely by the relative dielectric permittivity, $K = [(1 + R^{1/2})/(1 - R^{1/2})]^2$; the bulk density d can then be estimated from $K = 1.9^d$. The last expression has been shown (Olhoeft, 1979; Olhoeft and Strangway, 1975) to have an rms fractional error of less than 0.2 for dry, nonmetallic rocks.

Applying these formulas to the Ra-Shalom data we find that the magnitude of the observed variations in σ_{OC} can be explained by an approximately twofold variation in the disc-averaged density of the surface regions visible at the observed rotational phases. Furthermore, the least dense regions probably have $d > 0.7$ g cm^{-3}; if their porosity (i.e., pore fraction) is 0.6 [corresponding to the uppermost 5 to 10 cm of some of the more porous lunar core samples (Carrier *et al.*, 1973)], then the solid material would have $d > 1.7$ g cm^{-3}. This constraint (which rests on a concatenation of many assumptions!) is consistent with a host of plausible surface compositions, including mineralogical analogs of C2/C3 meteorites, whose densities are typically within 10% of 3 g cm^{-3} (Buchwald, 1975) and whose VIS/IR spectral reflectances resemble those of Ra-Shalom (McFadden, 1983).

The relatively large estimate of σ_{OC} on Aug 26 might also be explicable in terms of geometrical effects on a scale much larger than the radar wavelength. If Ra-Shalom's gross shape is curved less on the side facing Earth during the left-hand lightcurve maxi-

mum (Fig. 4c) than it is on the opposite side, and if the scattering is far from "geometric," then σ_{OC} and p might surge for rotational phases presenting the flatter side. One could interpret the variations in single-run estimates of σ_{OC} on Aug 26 (see Sect. II) as evidence in favor of this hypothesis. In any event, the radar data seem difficult to reconcile with a homogeneously scattering, axisymmetric model.

V. CONCLUSION

Our radar and photoelectric results are consistent with Ra-Shalom having a rotation period of about 20 hr, largest dimensions of about 3 km, a somewhat irregular shape, and heterogeneous decimeter-scale surface properties. However, given the ambiguities in the estimate of P_{syn}, any values inferred from our radar bandwidth estimates for Ra-Shalom's dimensions (and hence for optical albedo, normalized radar cross section, surface density, etc.) remain provisional. Intensive radar, photoelectric, and infrared radiometric observations are planned for Ra-Shalom during its summer 1984 apparition, and are expected to refine substantially our constraints on this asteroid's physical properties.

ACKNOWLEDGMENTS

We thank B. Marsden for providing information useful in the preparation of the radar ephemerides; A. Forni for calculation of those ephemerides; R. Velez and the staff of the Arecibo Observatory for assistance with the radar observations; J. Gibson for assistance with observations at Table Mountain; C. Ikuta and M. Roth for secretarial assistance; E. Bowell, D. Tholen, and E. Tedesco for providing their unpublished observations; L. Lebofsky and G. Veeder for discussions of radiometric techniques; and R. E. McCrosky, R. A. Simpson, E. F. Tedesco, and D. Tholen for valuable comments on an earlier version of this paper. This research was supported in part by NASA Grant NAGW-116 (Ostro) and in part by NSF Grant PHY78-07769 (Shapiro). The work at Table Mountain Observatory and at the Jet Propulsion Laboratory, Caltech, was supported under contract from NASA. The Arecibo Observatory is part of the National Astronomy and Ionosphere Center.

REFERENCES

BOWELL, E., AND K. LUMME (1979). Colorimetry and magnitudes of asteroids. In *Asteroids* (T. Gehrels, Ed.). Univ. of Arizona Press, Tucson.

BROWN, R. H., D. MORRISON, C. M. TELESCO, AND W. E. BRUNK (1982). Calibration of the radiometric asteroid scale using occultation diameters. *Icarus* **52,** 188–195.

BUCHWALD, V. F. (1975). *Handbook of Iron Meteorites,* p. 62. Univ. of California Press, Berkeley.

CARRIER, W. D., III, J. J. MITCHELL, AND A. MAHMOOD (1973). *Proceedings of the Fourth Lunar Science Conference,* pp. 2403–2411. Pergamon, Elmsford, N.Y.

CHANDRASEKHAR, S. (1960). *Radiative Transfer.* Dover, New York.

EVANS, J. V., AND G. H. PETTENGILL (1963). The scattering behavior of the Moon at wavelengths of 3.6, 68, and 784 centimeters. *J. Geophys. Res.* **68,** 423–446.

FRENCH, L. M., AND J. VEVERKA (1983). Limb darkening of meteorites and asteroids. *Icarus* **54,** 38–47.

GEHRELS, T., AND E. F. TEDESCO (1979). Minor planets and related objects. XXVIII. Asteroid magnitudes and phase relations. *Astron. J.* **84,** 1079–1087.

HAGFORS, T. (1968). Radar studies of the Moon. In *Radar Astronomy* (J. V. Evans and T. Hagfors, Eds.). McGraw-Hill, New York.

HAPKE, B. (1981). Bidirectional reflectance spectroscopy. I. Theory. *J. Geophys. Res.* **86,** 3039–3054.

HARRIS, A. W., J. W. YOUNG, F. S. SCALTRITI, AND V. ZAPPALÀ (1984). Lightcurves and phase relations of the asteroids 82 Alkmene and 444 Gyptis. *Icarus* **57,** 251–258.

HARRIS, A. W., AND J. W. YOUNG (1983). Asteroid rotation. IV. 1979 observations. *Icarus* **54,** 59–109.

HELIN, E. F., E. M. SHOEMAKER, AND R. F. WOLFE (1978). Ra-Shalom: Third member of the Aten class of Earth-crossing asteroids. *Bull. Amer. Astron. Soc.* **10,** 732.

JOHNSON, H. L., AND W. W. MORGAN (1953). Fundamental stellar photometry for standards of spectral type on the revised system of the Yerkes Spectral Atlas. *Astrophys. J.* **117,** 313–352.

JURGENS, R. F., AND R. M. GOLDSTEIN (1976). Radar observations at 3.5 and 12.6 cm wavelength of asteroid 433 Eros. *Icarus* **28,** 1–15.

LANDOLT, A. U. (1983). UBVRI photometric standard stars around the celestial equator. *Astron. J.* **88,** 439–460.

LANDOLT, A. U. (1973). UBV photoelectric sequences in the celestial equatorial selected areas 92–115. *Astron. J.* **78,** 959–1020.

LEBOFSKY, L. A., G. J. VEEDER, AND D. L. MATSON (1984). Private communication.

LEBOFSKY, L. A., G. J. VEEDER, M. J. LEBOFSKY, AND D. L. MATSON (1978). Visual and radiometric photometry of 1580 Betulia. *Icarus* **35,** 336–343.

LUMME, K., AND E. BOWELL (1981a). Radiative transfer in the surfaces of atmosphereless bodies. I. Theory. *Astron. J.* **86,** 1694–1704.

LUMME, K., AND E. BOWELL (1981b). Radiative transfer in the surfaces of atmosphereless bodies. II. Interpretation of phase curves. *Astron. J.* **86,** 1705–1721.

MCFADDEN, L. A. (1983). *Spectral Reflectances of Near-Earth Asteroids: Implications for Composition, Origin and Evolution.* Ph.D. thesis, University of Hawaii.

MINNAERT, M. (1941). The reciprocity principle in lunar photometry. *Astrophys. J.* **93,** 403–410.

OLHOEFT, G. R. (1979). *Tables of Room Temperature Electrical Properties for Selected Rocks and Minerals with Dielectric Permittivity Statistics.* U.S. Geological Survey Open File Report 79-993.

OLHOEFT, G. R., AND D. W. STRANGWAY (1975). Dielectric properties of the first 100 meters of the Moon. *Earth Planet. Sci. Lett.* **24,** 394–404.

OSTRO, S. J., D. B. CAMPBELL, AND I. I. SHAPIRO (1981). Radar detection of Iris, Psyche, Klotho, Apollo, and Quetzalcoatl. *Bull. Amer. Astron. Soc.* **13,** 716.

OSTRO, S. J., D. B. CAMPBELL, AND I. I. SHAPIRO (1983). Radar observations of asteroid 1685 Toro. *Astron. J.* **88,** 565–576.

OSTRO, S. J., AND R. CONNELLY (1984). Convex profiles from asteroid lightcurves. *Icarus* **57,** 443–463.

SHOEMAKER, E. M., J. G. WILLIAMS, E. F. HELIN, AND R. F. WOLFE (1979). Earth-crossing asteroids: Orbital classes, collision rates with Earth, and origin. In *Asteroids* (T. Gehrels, Ed.). Univ. of Arizona Press, Tucson.

TEDESCO, E. F., J. DRUMMOND, M. CANDY, P. BIRCH, I. NIKOLOFF, AND B. ZELLNER (1978). 1580 Betulia: An unusual asteroid with an extraordinary lightcurve. *Icarus* **35,** 344–359.

VEVERKA, J., J. GOGUEN, S. YANG, AND J. L. ELLIOT (1978). Near-opposition limb-darkening of solids of planetary interest. *Icarus* **33,** 368–379.